Neutral and Charged Current Neutrino-Nucleus Coherent Measurements

H. Gallagher[*], D.Harris[†], A. Kartavtsev[‡] and E. Paschos[§]

MINERνA Note 300
October, 2004

Abstract

Coherent neutrino-nucleus scattering via both the charged and neutral currents can be studied with unprecedented precision by MINERνA. In this note we will summarize several preliminary studies to estimate the signal and background amounts in neutral and charged-current analyses for varying nuclei. The high statistics, range of nuclear materials, fine granularity, strong pattern recognition capabilities, and good electromagnetic calorimetry of the MINERνA detector make it ideal for a number of measurements related to the charged and neutral-current coherent processes.

1 Introduction

The MINERνA experiment has the potential to improve dramatically our knowledge of the dynamics of coherent neutrino-nucleus scattering. This process, in which the neutrino scatters coherently from the entire nucleus with small energy transfer, leaves a relatively clean experimental signature and has been studied in both charged-current ($\nu_\mu + A \rightarrow \mu^- + \pi^+$) and neutral-current ($\nu_\mu + A \rightarrow \nu + \pi^o$) interactions of neutrinos and anti-neutrinos. Although the interaction rates are typically an order of magnitude or more lower than other single-pion production mechanisms, the distinct kinematic characteristics of these events allow them to be identified. Because the outgoing pion generally follows the incoming neutrino direction closely, this reaction is an important background to searches for $\nu_\mu \rightarrow \nu_e$ oscillation, as these events can easily mimic the oscillation signature of a single energetic electron shower. Neutral-current coherent production will be discussed in more detail in Section 3.3; here we limit our attention to the charged-current channel where the kinematics can be fully measured and the underlying dynamics explored.

[*]Tufts University
[†]Fermilab
[‡]Rostov State University
[§]University of Dortmund

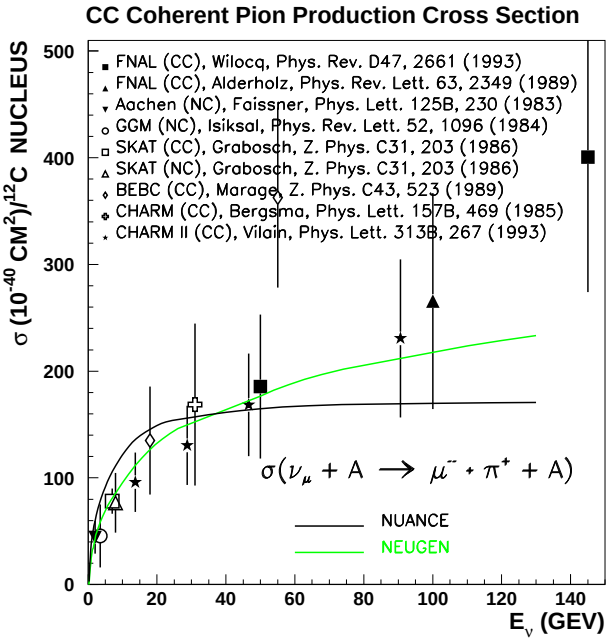

Figure 1: Charged-current neutrino–carbon coherent cross-sections. Results have all been scaled to carbon assuming an $A^{1/3}$ dependence, and $\sigma(CC) = 2\sigma(NC)$ [1].

2 Theory

It is well known from electron scattering that at low Q^2 and high ν, vector mesons are abundantly produced through diffractive mechanisms. These interactions are interpreted as fluctuation of the virtual photon intermediary into a virtual meson with the same quantum numbers, which by the uncertainty principle can travel a length

$$l \sim \frac{\nu}{Q^2 + m^2} \tag{1}$$

where m is the mass of the meson in question. For the weak current, similar fluctuations can occur, into both vector- and axial-vector mesons. From the Adler relation and "partially-conserved axial current" (PCAC) hypothesis, it is known that the hadronic current at low Q^2 is proportional to the pion field. The hadronic properties of the weak current in these kinematic regions have been investigated through the study of nuclear shadowing at low x and the coherent production of π, ρ, and a_1 mesons. Coherent scattering therefore allows investigation of the PCAC hypothesis and hadron dominance models of the weak current in detail [2].

A number of calculations of coherent scattering, involving substantially different procedures and assumptions, have been made over the past thirty years[3, 4, 5, 6]. These calculations factorize the problem in terms of the hadron-like component of the weak current and the scattering of this hadron with the nucleus. The calculations assume PCAC as a starting point but quickly diverge when it comes to the number of hadronic states required to describe the weak current and how

the hadron–nucleus scattering should be treated. The Rein-Sehgal model, used by both NUANCE and NEUGEN, describes the weak current only in terms of the pion field; the Q^2 dependence of the cross-section is assumed to have a dipole form. Other calculations rely on meson-dominance models[5] which include the dominant contributions from the ρ and a_1 mesons. Figure 1 shows the coherent charged-current cross-section as a function of energy, compared to the model by Rein and Sehgal as implemented in NEUGEN and the calculation in [6].

3 Experimental Studies of Coherent Production

The MINERνA experiment, with its high statistics wide band beam, excellent pattern recognition capabilities, good electromagnetic calorimetry, and variety of nuclear targets, has the potential to greatly improve our experimental understanding of coherent reaction processes. As described in previous documents, the variety of nuclear targets - from carbon to lead - in MINERνA make possible a detailed measurement of the A dependence of the coherent cross section. An additional strength of the experiment is its strong pattern recognition capabilities for both the neutral-current and charged-current channels. Identified samples of charged-current coherent events can be used to study the differential cross sections for coherent scattering. Comparions of the overall rates of neutral and charged-current production, as well as comparison of the pion energy and angular distributions from neutral-current and charged-current events will also provide useful tests of the various models. For several recent models, the prediction for the CC/NC ratio in coherent scattering differs by around 20% [3, 6].

The topic of comparing charged and neutral-current coherent production is of significant current interest. In the low energy range there is very limited data on either process from bubble chamber experiments, and data from the K2K and miniBoone experiments is only now exploring at least the neutral-current process at $\sim$ 1 GeV in carbon and oxygen. While data on single π^o production from these experiments are in reasonable agreement with the predictions [7, 8], the study of the charged-current process is limited because of detector capabilities and hampered by the fact that the Q^2 distribution for inelastic events (or all events where quasi-elastic and inelastic cannot be separated with high efficiency) shows a strong depletion at low Q^2 compared with the Monte Carlo predictions [9, 10]. Numerous explanations for this low Q^2 suppression have been put forward [11, 12]. Since coherent events are at low Q^2, they have been under scrutiny as a possible contributor to the disagreement. Empirically it has been noted that the discrepancy could be largely addressed by eliminating charged-current coherent interactions from the Monte Carlo. While this drastic suggestion is certainly not physically warranted, it does raise questions about the charged-current coherent process in the several-GeV region. In this section we will summarize the simulations which have been carried out on coherent interactions in MINERνA

3.1 Charged Current Cross Section

The kinematics of coherent scattering are quite distinct compared to the more common deep-inelastic and resonant interactions. Because the coherence condition requires that the nucleus

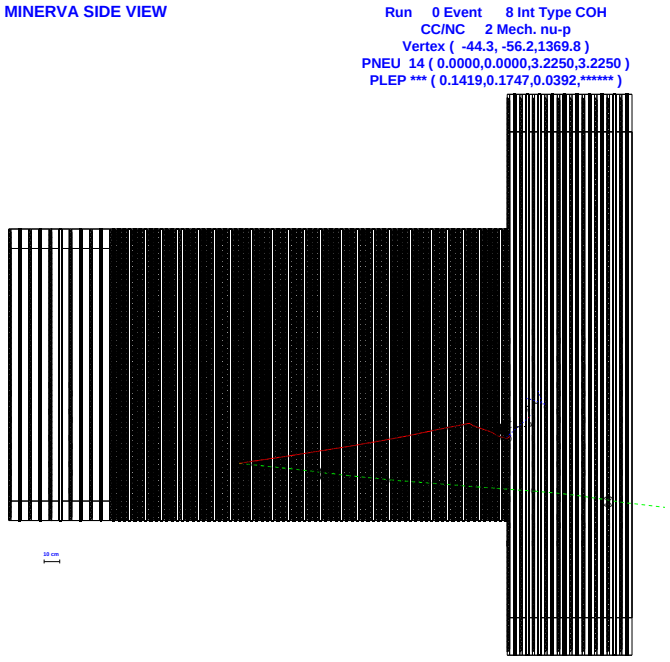

Figure 2: A charged-current coherent event in the inner tracking detector of MINERνA. For clarity the outer barrel detector is not shown.

remain intact, low-energy transfers to the nuclear system, $|t|$, are needed. Events are generally defined as coherent by making cuts on the number of prongs emerging from the event vertex followed by an examination of the t distribution, where t is approximated by:

$$-|t| = -(q - p_\pi)^2 = (\Sigma_i(E_i - p_i^{||}))^2 - (\Sigma_i(p_i^{\perp}))^2 \quad (2)$$

With its excellent tracking capabilities, the MINERνA inner detector can measure this kinematic variable well.

Figure 2 shows an event display of a coherent charged-current interaction in the MINERνA inner tracking detector. Distinct muon and pion tracks are clearly visible and the vertex location is well defined.

To determine the ability of the MINERνA experiment to measure the charged-current coherent cross section, a Monte Carlo study was carried out using the GEANT detector simulation described elsewhere in this proposal. Analysis cuts were tuned on a sample of coherent interactions corresponding to that expected in a 3 ton fiducial volume for the integrated 4 year run (24630 events). Events were generated according to the appropriate mix of low, medium, and high energy running. This study used the Rein-Seghal [3] model of coherent production, as implemented in NEUGEN3. A 20k low-energy beam event sample was used for background determination. This sample included the appropriate mix of neutral and charged-current events. Based on published bubble chamber analyses, it is expected that charged-current reactions are the largest contributor to background processes, in particular quasi-elastic and delta production reactions where the baryon

Experiment	Reaction	Energy (GeV)	A	Signal	Ref
Aachen-Padova	NC	2	27	360	[13]
Gargamelle	NC	2	30	101	[14]
CHARM	NC	20-30	20	715	[15]
CHARM II	CC	20-30	20	1379	[16]
BEBC (WA59)	CC	5-100	20	158	[17, 18]
SKAT	CC (NC)	3-20	30	71 (14)	[19]
FNAL 15'	NC	2-100	20	28	[20]
FNAL 15' E180	CC	10-100	20	61	[21]
FNAL 15' E632	CC	10-100	20	52	[22]

Table 1: Existing measurements on coherent pion production[2].

is not observed or is misidentified as a pion. To isolate a sample of coherent interactions, a series of cuts are placed on event topology and kinematics.

Topological Cuts: an initial set of cuts are applied to isolate a sample of events which contain only a muon and charged pion. These cuts are based on the hit-level and truth information as provided by the GEANT simulation.

1. **2 Charged Tracks:** The event is required to have 2 visible charged tracks emerging from the event vertex. A track is assumed to be visible if it produces at least 8 hit strips in the fully active region of the detector which are due to this track alone.

2. **Track Identification:** The two tracks must be identified as a muon and pion. The muon track is taken to be the most energetic track in the event which does not undergo hadronic interactions. The pion track is identified by the presence of a hadronic interaction. The pion track is required not to have ionization characteristic of a stopping proton (which is assumed can be identified 95% of the time).

3. π^o**/neutron Energy:** Because the MINERνA detector is nearly hermetic we have also assumed that neutral particles will produce visible activity which can be associated with the event and cause it to be identified as not coherent. Events with more than 500 MeV of neutral energy (π^o or neutron) produced in the initial neutrino interaction are rejected.

4. **Track Separation:** In order to make good measurements of the two tracks, it is required that the interaction point of the pion be greater than 30 cm from the vertex and that, at this interaction point, at least 4 strips separate the two tracks in at least one view.

Kinematic Cuts: because of the very different kinematics between coherent and background reactions, cuts on kinematic variables are very effective at isolating the final sample. In this analysis, the true pion and muon 4-momenta were used as the reconstruction values. For the final event rates we reduce our overall signal sample by 0.65 to roughly account for this assumption. The difference between true and reconstructed variables obviously depends strongly on the pattern recognition and

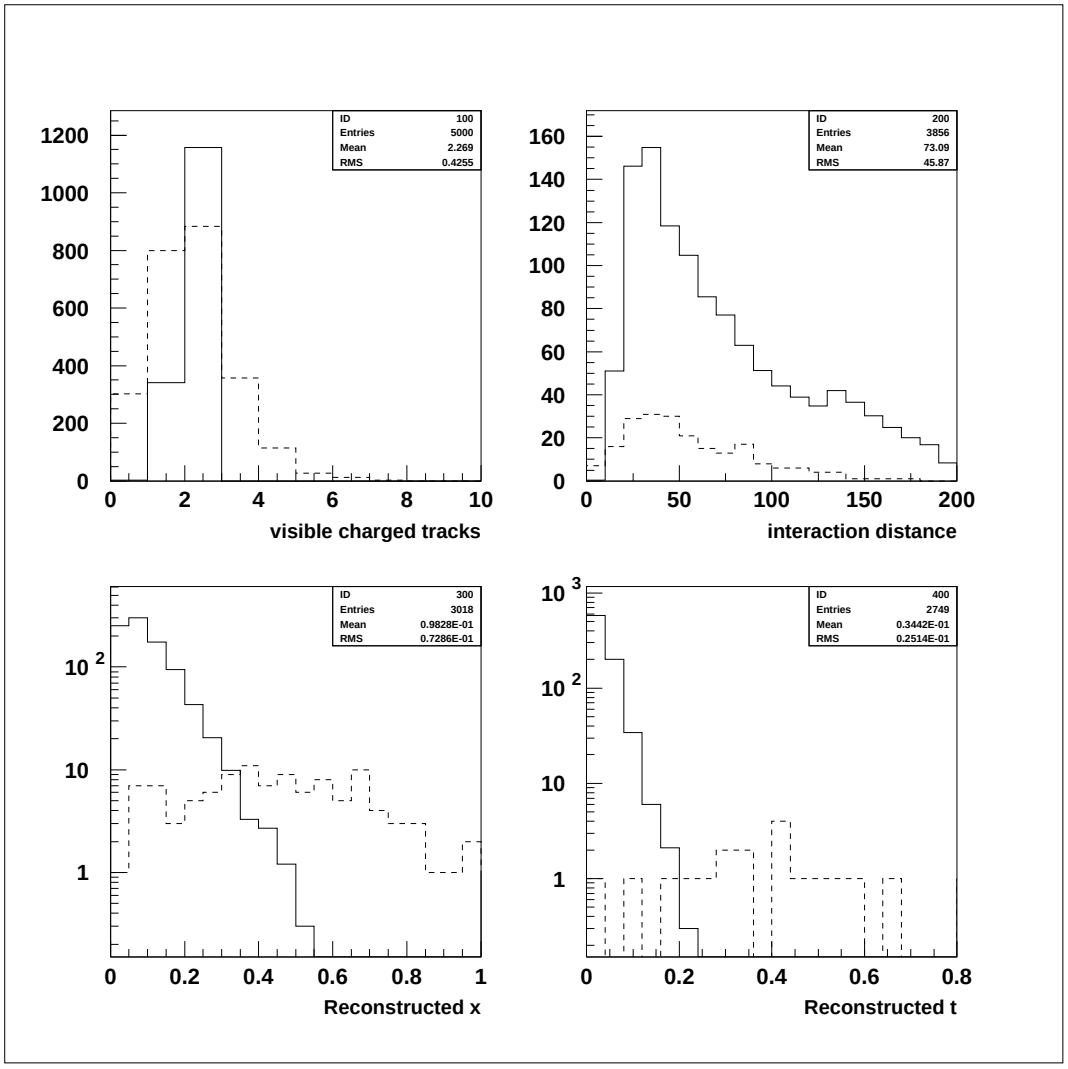

Figure 3: Topological and kinematic quantities used to define the coherent sample. In all plots the solid histogram is the coherent sample and the dashed histogram are background processes. The relative normalizations of the two distributions in the initial plot is arbitrary, subsequent plots show the effect of the applied cuts. Top Left: Visible charged tracks. Top Right: Distance between the event vertex and the location of the pion interaction (in cm). Bottom Left: Bjorken-x as computed from the true pion and muon 4-momenta. Bottom Right: Square of the 4-momentum transfer to the nucleus (in GeV^2) as calculated from the pion and muon 4-momenta.

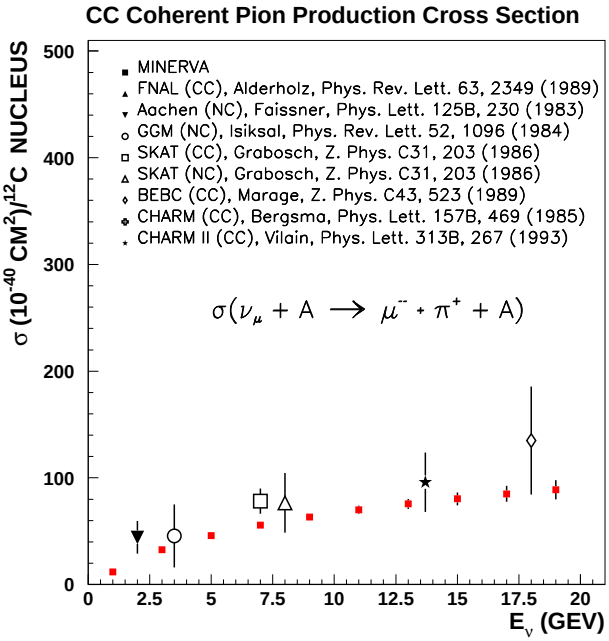

Figure 4: Coherent cross-sections as measured by MINERνA compared with existing published results. MINERνA errors here are statistical only.

reconstruction capabilities of the detector, and this value is thought to not be unreasonable for the reconstruction of the event kinematics for coherent events. This statement is based partly on the fact that the event topologies lend themselves to reconstruction of individual tracks, for which the angular resolution is quite good, and that the energy resolution for single pions is likely to be significantly better than that obtained for neutrino-induced hadron showers. Figure 10 shows the true and reconstructed angular distributions for neutral pions produced via the neutral-current reaction, in this case the difference between truth and reconstructed quantities is minimal.

1. **x**< 0.2**:** A cut is made requiring that Bjorken-x (as reconstructed from the observed pion and muon 4-momenta) be less than 0.2. This cut eliminates a large amount of the background coming from quasi-elastic reactions which have x$\sim$1.

2. **t**< 0.2**GeV**^{2}**:** The most powerful variable for the identification of coherent events is the square of the 4-momentum transfer to the nucleus. Equation 2 relating t to the observed particles in the event is used as the estimator of this quantity.

3. $p_\pi >$ **600 MeV:** Requiring $p_\pi > 600$ MeV effectively eliminates backgrounds from delta production which tend to produce lower energy pions.

The cummulative effect of these cuts on the signal and background samples is shown in Table 3.1, and the signal and background distributions for several of the important cut variables are shown in Figure 4.

Cut	Signal Sample	Background Sample
	5000	10000
2 Charged Tracks	3856	3693
Track Identification	3124	3360
π^o/neutron Energy	3124	1744
Track Separation	2420	500
x<0.2	2223	100
t<0.2	2223	19
$p_\pi < 600$ MeV	1721	12

Table 2: Analysis cuts to isolate a sample of coherent interactions. The cuts are described in the text.

Applying this set of cuts to our signal sample we find that 7698 signal events pass all cuts, which gives an overall efficiency of 31%. Applying the factor 0.65 to account for the fact that we have not used fully reconstructed quantities for our kinematic cuts gives us a final event sample of 5004 events. Applying these cuts to the background sample we find that 12 events out of 20k pass all cuts. Normalized to the total event rate this gives an expected background of 4400 events. We note that in this analysis other important variables for background rejection, related to associated activity around the vertex, were not used. Figure 4 shows the expected precision of the MINERνA measurement as a function of neutrino energy. Here we have only included the statistical error on the signal and assumed that the measured value is that predicted by Rein-Seghal. An attempt has not been made to quantify the systematic errors on this measuerment other than that resulting from the background subtraction. Previous measurements of the coherent cross section were statistics limited.

3.2 A-Dependence of the Cross Section

Another task for MINERνA will be comparison of reaction rates for lead and carbon. The expected yield from lead will be $\approx$ 1800 charged-current events, assuming the same efficiency. The A dependence of the cross-section depends mainly on the model assumed for the hadron–nucleus interaction, and serves as a crucial test for that component of the predictions. No experiment to date has been able to perform this comparison. For reference, the predicted ratio of carbon to lead neutral-current cross-sections at 10 GeV in the Rein-Sehgal and Paschos models are 0.223 and 0.259, respectively [23]. Figure 5 shows the predicted A-dependence according to the model of Rein and Sehgal.

3.3 Neutral Current Cross Section

Neutral-current π^0 production can occur through a number of mechanisms - resonant production, coherent production, and deep-inelastic scattering. Figure 7 shows a striking example of

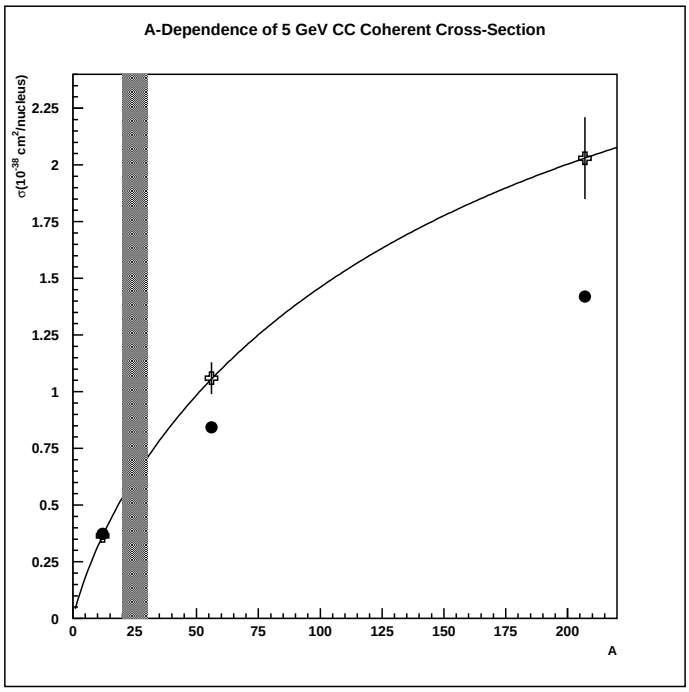

Figure 5: Measurement of the coherent cross section as a function of atomic number in MINERνAṪhe shaded band indicates the range of previous measurements. Error bars indicate the size of the experimental errors in a single 1-GeV bin. The curve shows the prediction from the Rein-Seghal model. Crosses are the prediction of the Rein-Seghal model for scattering from carbon, iron, and lead, circles are the predictions of the Paschos-Kartavtsev model.

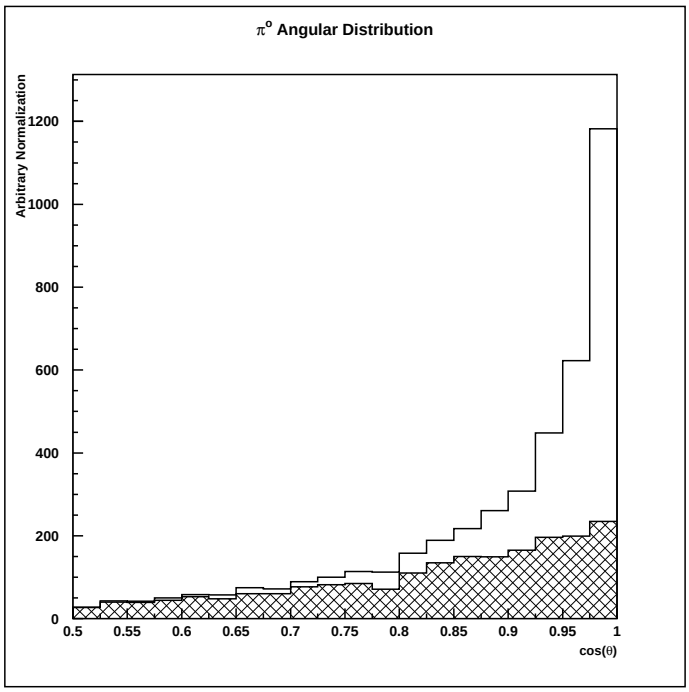

Figure 6: Neutral-current single π^0 angular distribution with respect to the beam for a flat neutrino flux between 1 and 11 GeV. Thelarger histogram shows the contribution from coherent and resonant prouction, while the dhatched histogram corresponds to the contribution from resonant production only, where the pion carries more than 80% of the total energy.

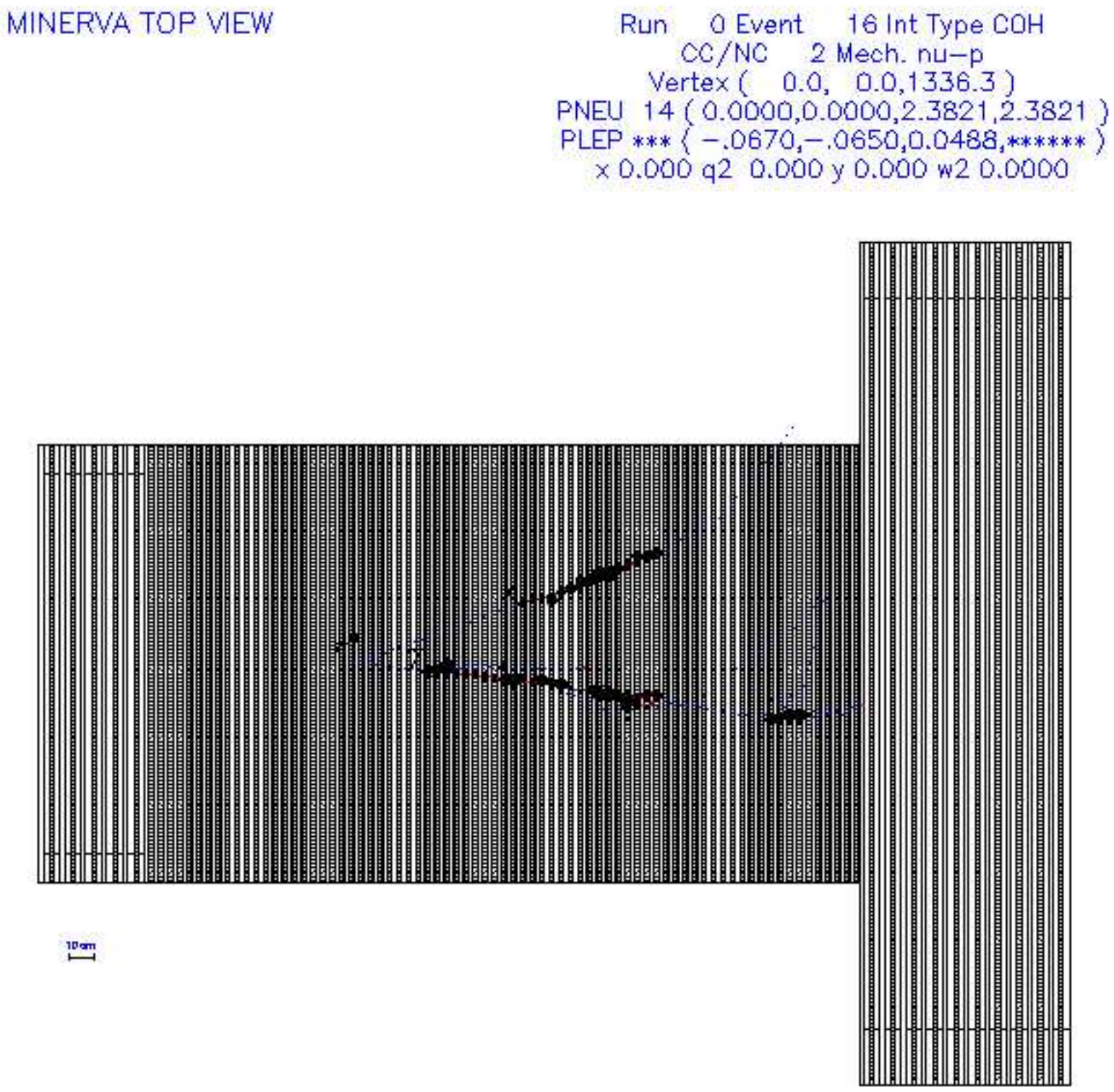

Figure 7: A simulated neutral-current coherent π^0 production event in MINERνA. The position of the $\pi 0$ decay vertex can be determined accurately by extrapolating the two photons backward. Notice that both photons pass through a number of planes before beginning to shower, distinguishing them from electrons.

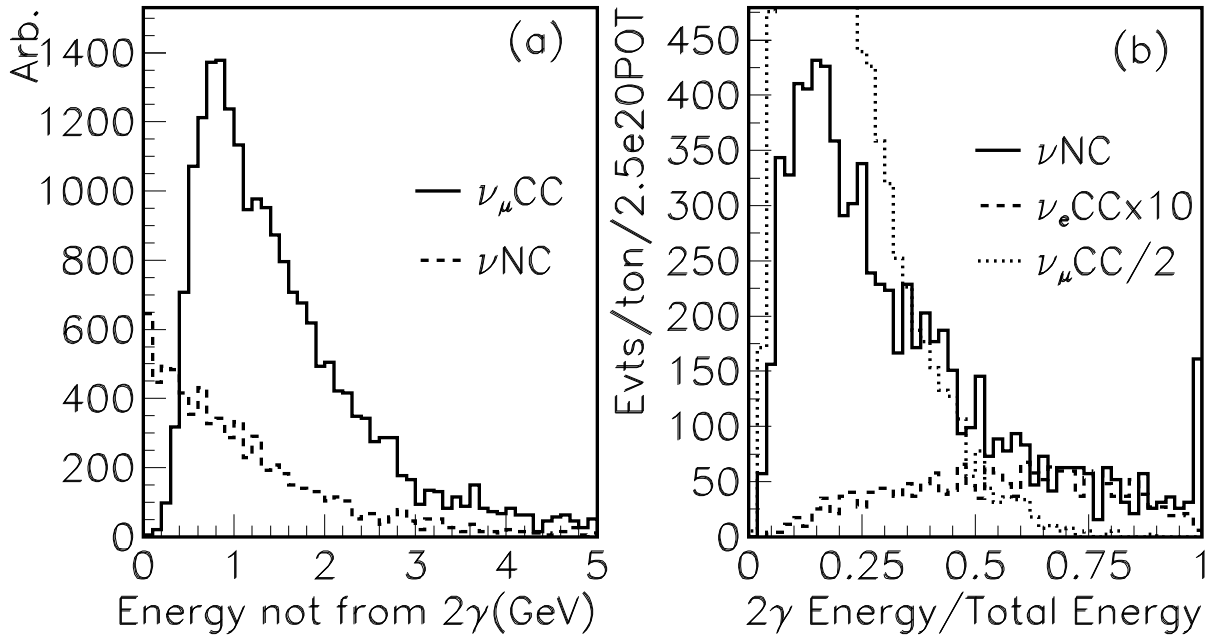

Figure 8: Variables that reject backgrounds to coherent π^0 measurements: (a) Other energy in the event for ν_μ Charged and neutral-current events, and (b) Ratio of two photon energy to total event energy for ν_μ charged-current sample (reduced by factor of 2), ν_e charged-current (increased by a factor of 10) and the neutral-current sample (normalized per ton per year, acceptance calculated for 3 tons fiducial volume)

MINERνA's response to coherent π^0 production.

By requiring two well-separated electromagnetic clusters that shower in the scintillator target, and extend at least 6 scintillator planes, one can keep about 30% of the coherent π^0 events that are produced in the detector. Furthermore, by requiring the ratio of the energy in the two clusters to that of the total event energy to be above 90%, and requiring any extra energy to be below 100MeV, one can reduce both the ν_e (ν_μ) charged-current contamination to a few (less than one) events. Figure 8 shows these two last variables, where the coherent $\pi 0$ peak is clearly visible in the plot on the right. The resulting sample in this simple analysis (1000 events per year in 3 tons of fiducial mass) is roughly half resonant π^0 production and half coherent π^0 events, which can be separated by studying the angular and energy distribution of the events, as well as the presence or absence of additonal particles at the production vertex identified by the two photon showers.

Neutral pions from resonance decay are not as energetic or collinear as those produced coherently. Resonant π^0 are particularly susceptible to final-state nuclear interaction and rescattering, which will be studied in detail by MINERνA using charged-current reactions.

As a proof-of-concept, a sample of neutral-current single-π^0 events has been selected using simple cuts. For events with two well-separated electromagnetic clusters ($E_\pi \equiv E_1 + E_2$), each passing through at least six planes of the fully-active region, requiring $E_\pi/E_{tot} > 90\%$ and $E_{tot} -$

$E_\pi < 100$ MeV efficiently isolates a neutral-current π^0 sample, as shown in Figure 9. After these cuts, the contamination of ν_e and ν_μ charged-current interactions (combined) is less than 1%. The resulting sample contains about 2400 neutral-current π^0 events per 3 ton-yr, of which half are resonant and half coherent.

Coherent and resonant interactions can be cleanly separated by cutting on the π^0 angle to the beam direction, as shown in Figure 10, which also highlights MINERνA's excellent π^0 angular resolution. The overall efficiency for selecting coherent neutral-current π^0 is about 40%.

References

[1] G. P. Zeller, (2003), hep-ex/0312061.

[2] B. Z. Kopeliovich and P. Marage, Int. J. Mod. Phys. **A8**, 1513 (1993).

[3] D. Rein and L. M. Sehgal, Nucl. Phys. **B223**, 29 (1983).

[4] A. A. Belkov and B. Z. Kopeliovich, Sov. J. Nucl. Phys. **46**, 499 (1987).

[5] C. A. Piketty and L. Stodolsky, Nucl. Phys. **B15**, 571 (1970).

[6] E. A. Paschos and A. V. Kartavtsev, (2003), hep-ph/0309148.

[7] Super-Kamiokande and K2K, C. Mauger, Nucl. Phys. Proc. Suppl. **112**, 146 (2002).

[8] BooNE, J. L. Raaf, (2004), hep-ex/0408015.

[9] MiniBooNE, J. Monroe, (2004), hep-ex/0408019.

[10] K2K, T. Ishida, Prepared for 1st Workshop on Neutrino - Nucleus Interactions in the Few GeV Region (NuInt01), Tsukuba, Japan, 13-16 Dec 2001.

[11] H. Budd, A. Bodek, and J. Arrington, (2003), hep-ex/0308005.

[12] B. Z. Kopeliovich, (2004), hep-ph/0409079.

[13] H. Faissner *et al.*, Phys. Lett. **B125**, 230 (1983).

[14] E. Isiksal, D. Rein, and J. G. Morfin, Phys. Rev. Lett. **52**, 1096 (1984).

[15] CHARM, F. Bergsma *et al.*, Phys. Lett. **B157**, 469 (1985).

[16] CHARM-II, P. Vilain *et al.*, Phys. Lett. **B313**, 267 (1993).

[17] BEBC WA59, P. P. Allport *et al.*, Z. Phys. **C43**, 523 (1989).

[18] BEBC WA59, P. Marage *et al.*, Z. Phys. **C31**, 191 (1986).

[19] SKAT, H. J. Grabosch *et al.*, Zeit. Phys. **C31**, 203 (1986).

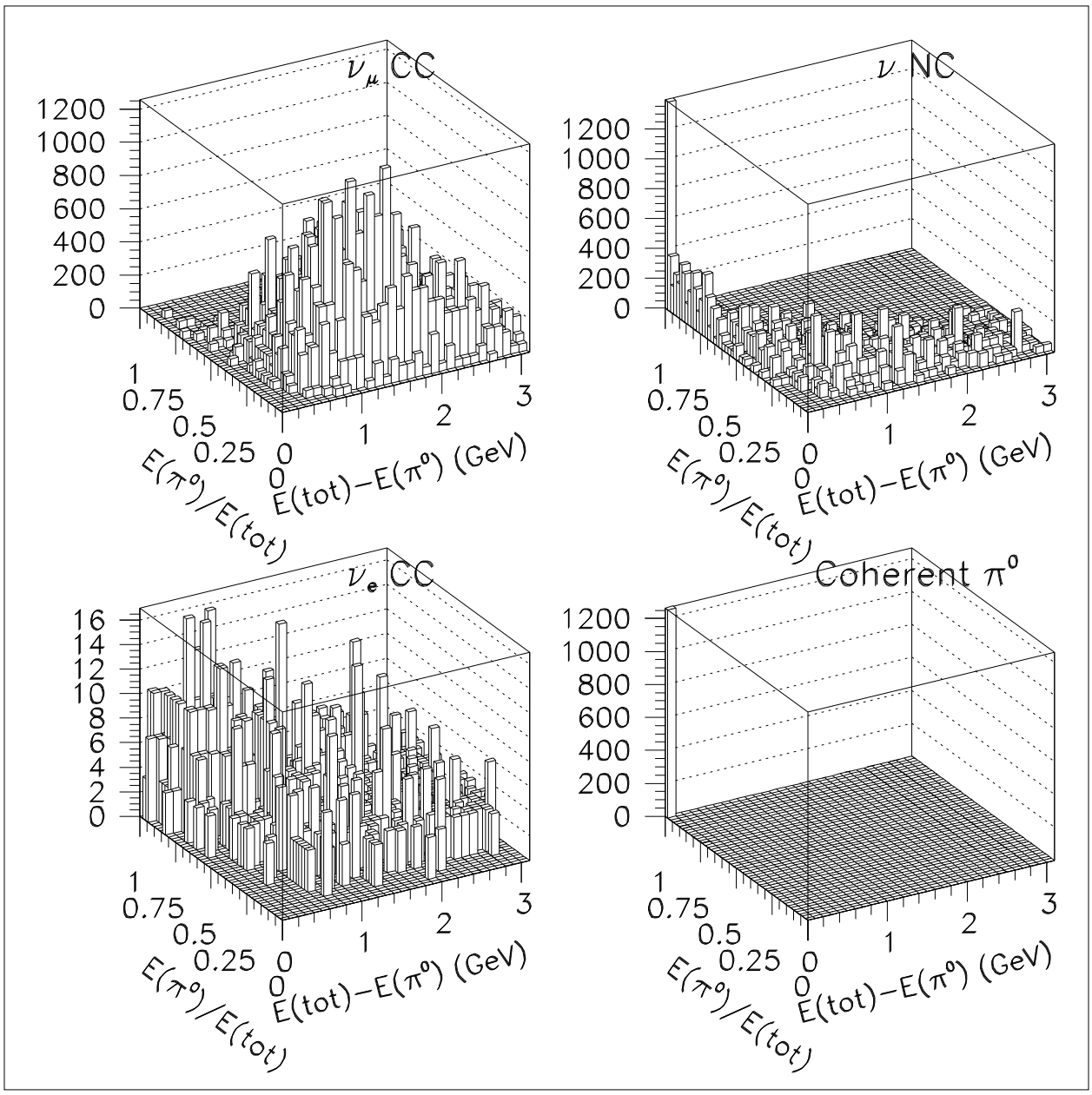

Figure 9: Selection of neutral-current single-π^0 production. The variables plotted are the fraction of visible energy carried by the π^0 candidate (E_π/E_{tot}) and the residual energy $E_{tot} - E_\pi$. The left-hand plots show the backgrounds from ν_μ(top) and ν_e(bottom). The plot at top right shows the same distribution for true neutral-current π^0 production, and the lower right shows the subset from coherent scattering. In the neutral-current plots, notice the dramatic concentration of the coherent π^0 signal in a single bin, in the left-most corner of the graph. All samples shown are normalized to a 3 ton-yr exposure of MINERνA.

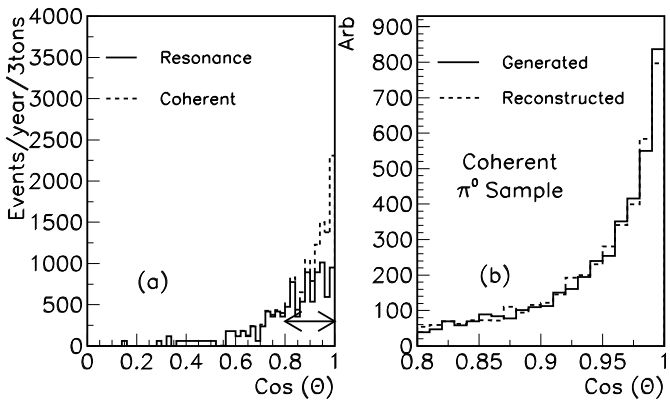

Figure 10: Angular distribution of neutral-current single-π^0 sample. The plot at left shows all events passing the cuts on E_π/E_{tot} and $E_{tot} - E_\pi$ described in the text, broken down into coherent and resonant reactions. The coherent sample is strongly forward-peaked. The plot at right is a close-up of the forward region comparing the true and reconstructed π^0 angular distributions from the beam direction. The distributions are nearly identical, highlighting the MINERνA's excellent angular resolution.

[20] C. Baltay *et al.,* Phys. Rev. Lett. **57**, 2629 (1986).

[21] V. V. Ammosov *et al.,* Yad. Fiz. **45**, 1662 (1987).

[22] E632, S. Willocq *et al.,* Phys. Rev. **D47**, 2661 (1993).

[23] E. Paschos and A. Kartavtsev, Private Communication.